






Green synthesis of silver nanoparticles and their bioactivities

Bolor Tsolmon¹ , Tsetseg-Erdene Tsevegkhasuren² , Nasantogtokh Oyunchimeg¹ ,
Suvdmaa Tuvaanjav² , Sarangerel Oidovsambuu¹ 

¹Institute of Chemistry and Chemical Technology, Mongolian Academy of Sciences, Ulaanbaatar 13330, Mongolia

²School of Art and Sciences, National University of Mongolia, Ulaanbaatar 14201, Mongolia

 Corresponding author: bolor_ts@mas.ac.mn; ORCID: <https://orcid.org/0000-0002-3404-0444>

Received: 14 July 2025; revised: 26 November 2025; accepted: 03 December 2025



ABSTRACT

Silver nanoparticles (AgNPs) were synthesized using aqueous extracts from three Mongolian wild berries: Blueberry (*Vaccinium uliginosum*), Lingonberry (*Vaccinium vitis-idaea*), and Sea buckthorn berry (*Hippophae rhamnoides*). The green synthesized AgNPs were characterized by UV-Vis, FTIR, SEM, and XRD analyses. UV-Vis peaks appeared at 410 nm (blueberry and lingonberry) and 445 nm (sea buckthorn). SEM showed spherical particles with average sizes of 32.36 ± 1.23 nm (Bb-AgNPs), 36.56 ± 7.86 nm (Lg-AgNPs), and 28.70 ± 1.38 nm (Sb-AgNPs). Zeta potential values ranged from -42.8 to -51.1 mV, indicating stable colloids. FTIR confirmed carboxylic acids, phenolics, and alcohols. Total phenolic contents were highest in blueberry extract (8.98 mg GAE/g). Bb-AgNPs showed notably higher antioxidant activity than the original extract. Both lingonberry extract and Lg-AgNPs demonstrated potential for antioxidant supplementation, with Lg-AgNPs also showing antibacterial properties.

Keywords: blueberry, lingonberry, sea buckthorn, aqueous extract, silver nanoparticle, green synthesis, antioxidant

INTRODUCTION

Green synthesis of silver nanoparticles (AgNPs) is gaining momentum due to its numerous advantages over conventional methods, including eco-friendliness, cost-effectiveness, minimal downstream processing, and high yields. In plant extract-based synthesis, biological molecules such as carboxylic acids, vitamins, anthocyanins, flavonoids, and phenolic compounds not only reduce silver ions to nanoparticles but also serve as capping agents, stabilizing the formed nanoparticles. These capping agents help prevent nanoparticle agglomeration, reduce toxicity, and enhance biomedical activities. A synergistic effect between the metal core and these bioactive capping agents is expected, particularly when the agents themselves possess biological activity. Various fruit, seed, and leaf extracts have been explored for green synthesis, including extracts from blueberry leaves and fruits [1, 2], hawthorn [3], red currant [4], karonda berry [5], *solanum xanthocarpum* L. berries [6], roman berry [7], lingonberry [8], and both fruit and leaf extracts of sea buckthorn [9-11].

In Mongolia, blueberry (*Vaccinium uliginosum* L.), lingonberry (*Vaccinium vitis-idaea* L.), and sea

buckthorn berry (*Hippophae rhamnoides* L.) thrive in the northern and central regions, ripening in early autumn. Blueberries and lingonberries are nutrient-rich and contain numerous bioactive compounds with potent antioxidant properties [9]. Notably, Mongolian blueberries are particularly high in delphinidin-3-O-glycoside which have demonstrated antibacterial activity against various pathogens [5, 12].

Sea buckthorn berries are rich in lipids, anthocyanins, carotenoids, amino acids, unsaturated fatty acids, and phenolic compounds. All of these compounds exhibit a wide range of antioxidant, anti-inflammatory, and anticancer activities. Sea buckthorn berries also contain gallic acid and epigallocatechin gallate, which contribute to its antioxidant and antimicrobial properties [13, 14]. Lingonberries are rich in flavonol glycosides, anthocyanins, procyanidins, and flavan-3-ols, which demonstrate antimicrobial effects against bacteria such as *Streptococcus mutans* and *Fusobacterium nucleatum* [12]. Moreover, lingonberries exhibit high antioxidant capacity due to their rich content of chlorogenic acids and anthocyanins [15].

In this study, we aimed to synthesize silver nanoparticles (AgNPs) from aqueous extracts of

blueberry, lingonberry, and sea buckthorn berry, and to characterize the properties of the synthesized AgNPs. Additionally, we evaluated the antioxidative and antibacterial effects of the green-synthesized AgNPs in comparison to the aqueous extracts of the berries.

EXPERIMENTAL

Fully matured blueberries, lingonberries, and sea buckthorn berries were obtained from a local supermarket in Ulaanbaatar, Mongolia, in November 2022.

Silver nitrate was purchased from Tianjin Weichen Chemical Reagent Co., Ltd., China. 1,1-diphenyl-2-picrylhydrazyl (DPPH, purity \geq 98.0%), 2,2-azino-bis-(3-ethylbenzothiazoline-6-sulfonic acid) (ABTS, purity \geq 98.0%), and 2,4,6-tris(2-pyridyl)-s-triazine (TPTZ, purity \geq 98.0%) were purchased from Sigma Aldrich. Vitamin C and rutin (purity \geq 99.0%) were acquired from Alladin Industrial Corporation, Shanghai, China. All other reagents and solvents used were of analytical grade, and all aqueous solutions were prepared using freshly double-distilled water.

Preparation of the aqueous extracts from the berries: Ten grams of dried and ground berries were extracted with water in a 1:10 ratio, stirred for 30 minutes at room temperature, and allowed to stand for approximately 10 hours. The extraction process was repeated three times, after which the solvents were filtered using Whatman No.1 filter paper. The combined filtrates were then evaporated to powder in a vacuum evaporator at 50 °C under reduced pressure and stored at 4 ± 1 °C until further analysis. For the synthesis of AgNPs, these dried extracts were dispersed in deionized water at a final concentration of 0.2%.

Total carbohydrate content was determined by phenol sulfuric acid method [16] and total phenolic compound was determined by the Folin-Ciocalteu method [17].

To compare the chemical, physical, and biological properties, silver nanoparticles were synthesized using both green and chemical methods. In the green synthesis approach, aqueous berry extracts containing biological molecules served as natural reducing and stabilizing agents, whereas in the chemical synthesis method, trisodium citrate was employed as an artificial chemical reducing agent.

Green synthesis of AgNPs: Silver nitrate (20 mL; 1 mM) was added dropwise to 0.2% berry extracts (40 mL) with continuous stirring and heating at 40-50 °C on a magnetic stirrer. After 20-40 minutes, a color change in the solution indicated the formation of silver nanoparticles: Blueberry extract (Bb-AgNPs) changed from pink to dark brown, lingonberry extract (Lg-AgNPs) from pinkish to dark brown, and sea buckthorn extract (Sb-AgNPs) from colorless to brown. The resulting colloidal suspensions were centrifuged at 21,000 g for 30 minutes and the pellets obtained were re-dispersed in deionized water. To further purify the AgNPs by removing any adsorbed substances, the dispersion

and centrifugation steps were repeated two additional times. Finally, the synthesized nanoparticles were dried at room temperature.

Chemical synthesis of silver nanoparticles (chem-AgNP): To chemically synthesize silver nanoparticles (chem-AgNPs), a 1% trisodium citrate solution was used. Chem-AgNPs were prepared by adding 50 mL of a 1 mM AgNO₃ solution dropwise into 100 mL of the trisodium citrate solution, while stirring and heating at 40-50 °C on a magnetic stirrer. The mixture was continuously stirred and heated for one hour. Afterward, the solution was centrifuged at 4000 rpm for 40 minutes. The resulting precipitate was washed twice with deionized water, and dried at 50 °C.

Characterization of the AgNP: The UV-Vis spectra of all synthesized berry-derived nanoparticles and chemically synthesized nanoparticles were recorded using a Shimadzu UV-1600 PC spectrophotometer across a range of 200-800 nm, with a resolution of 5 nm. The spectra were compared to those of 1 mM AgNO₃ and a mixture of berry extracts (blueberry aqueous extract-BbAE, lingonberry aqueous extract-LgAE, and sea buckthorn aqueous extract-SbAE) with 1 mM AgNO₃. UV-Visible absorption spectra were obtained using quartz cuvettes with a 1 cm path length. FTIR analysis was performed using a Bruker Alpha II-FTIR model spectrometer, with results recorded in the range of 4000-400 cm⁻¹ at a temperature of 22 °C and humidity of 30%. The berry extracts were measured as dry samples, while the silver nanoparticles were analyzed in solution.

Zeta potential values of the AgNPs were measured using a Stabino zeta potential analyzer from Microtrac Retsch GmbH, Germany.

For X-ray diffraction analysis, the powdered sample was examined with a Cu-X-ray diffractometer (MAXima_X XRD-7000, Shimadzu) using Cu-K α radiation ($\lambda = 1.7903$ Å), operating at 40 kV and 30 mA. The diffraction pattern was recorded over a 2θ range of 10°–90° to confirm the presence of silver and to analyze the crystallite structure and size of the synthesized AgNPs. The polydispersity index (PDI) of all synthesized silver nanoparticles was calculated using the equation $PDI = (\sigma / D)^2$, where σ represents the standard deviation and D is the average particle diameter [18].

Antioxidant activity assays: The DPPH free radical scavenging activity was measured following a previously described method with minor modifications [19]. Briefly, the DPPH[•] solution was diluted with methanol to achieve an absorbance of 0.90 ± 0.02 at 517 nm. Then, 2 mL of various concentrations of AgNPs (0, 25, 50, 75, 100, 150, 200, and 500 μ g/mL) were mixed with 2 mL of DPPH[•] solution in glass tubes, vortexed, and incubated in the dark at room temperature for 30 minutes. Absorbance values were measured at 517 nm in quartz cuvettes with a 1 cm path length using a UV-1600 PC spectrophotometer. Methanol served as a negative control, while vitamin C and rutin were used

as positive controls.

The ABTS^{•+} scavenging assay was performed as previously described, with minor modifications [19]. The ABTS radical cation was generated by mixing 10.0 mL of ABTS stock solution (7.4 mM) with 10.0 mL of potassium persulfate (2.6 mM) and allowing the mixture to stand in the dark at room temperature for 12 hours. Before use, the ABTS^{•+} solution was diluted with deionized water to an absorbance of 0.70 ± 0.02 at 734 nm. To conduct the assay, 500 μ L of various concentrations of extracts (0, 25, 50, 75, 100, 150, 200, and 500 μ g/mL) were added to 3.5 mL of the ABTS^{•+} solution, vortexed, and kept in the dark at room temperature for 6 minutes. Absorbance values were measured at 734 nm in quartz cuvettes with a 1 cm path length using a UV-1600 PC spectrophotometer. Methanol served as a negative control, while vitamin C and rutin were used as positive controls.

Antibacterial activity: A total of six stock cultures of bacteria, including *Staphylococcus aureus* (ATCC 2592), *Pseudomonas aeruginosa* (ATCC 15442), *Escherichia coli* (ATCC 25922), *Enterococcus faecalis* (absent), *Bacillus subtilis* (ATCC 6633), and *Micrococcus luteus* (ATCC not available) were used to evaluate the antibacterial activity of the berry aqueous extracts and berries-AgNPs. A modified agar disk diffusion method was employed to determine the antibacterial efficacy of berries-AgNPs [10]. The synthesized silver nanoparticle solutions from berries were used directly for antibacterial activity. The bacteria stocks were subcultured with Nutrient broth as a liquid medium at 37 °C for 24 hours. Then, the bacterial liquid medium was inoculated in triplicate to obtain three samples of 100 μ L bacterial suspensions (final concentration of 1.5×10^8 CFU/mL bacteria). Next 25 mL agar nutrient was prepared and autoclaved for sterilization, and each sample of the bacterial suspension was swabbed onto an agar petri dish to cultivate a uniform microbial growth plate. Hollows were cut into the agar using sterile gel puncture, and 20 μ L of the prepared test solutions comprising berry-derived silver nanoparticle suspensions, 10 μ g/mL kanamycin as a positive control, distilled water, and 1 mM AgNO₃ as negative controls were poured into each well of the inoculated plates and incubated at 37 °C for 24 hours. To evaluate the antibacterial activity of the synthesized silver nanoparticles, the diameter of the inhibition zones were measured and compared with the control groups. Every assay of synthesized AgNPs from berries and controls (10 mg/ml kanamycin, distilled water and 1 mM AgNO₃) was carried out in triplicate. Antibacterial activity was indicated by the inhibition zone diameters (IZDs) standard deviation (SD) around the well and the results were reported as mean \pm standard.

Statistical analysis: All tests were done in triplicate, and mean values were reported with standard deviations. The IC₅₀ values were analyzed using GraphPad Prism 7 and Origin 2019b.

RESULTS AND DISCUSSION

Some chemical profile of Mongolian berries:

Assessing the therapeutic value of Mongolian wild berries is important for local communities due to their nutritional benefits, cultural heritage, and the potential for sustainable harvesting. In this study, we synthesized silver nanoparticles using aqueous extracts from three different types of Mongolian wild berries.

The yields of the aqueous extracts, total carbohydrate contents and total phenolic compounds of the berries are shown the Table 1. The total carbohydrate content in the aqueous extracts is quite a bit higher than that of berries grown in Belarus [14]. The total phenolic compounds in the aqueous extracts is also higher than in berries grown in Brazil [20].

Table 1. Some chemical profile of the Mongolian wild berries

Sample	Yield of the AE (%)	Total carbohydrate content (%)	Total phenolic compound (GAE mg/g)
Blueberry	16.79	15.16 \pm 1.22	8.98 \pm 0.037
Lingonberry	15.59	14.52 \pm 3.03	6.07 \pm 0.049
Sea buckthorn	17.29	9.62 \pm 1.37	3.65 \pm 0.037
In reference		9.9-11.9 [21]	3.0-14.6 [17, 21, 22]

Synthesis of the AgNPs: The formation of the AgNPs was initially verified by a color change of the AgNO₃ solution, it changed from colorless to dark brown. The alteration in color from the berry's own faint color to dark brown suspension verified the bioreduction process converting silver ions into AgNPs.

Figure 1 shows the UV-visible spectra of silver nanoparticles synthesized by chemical and green methods, including chem-AgNP (chemically synthesized), Bb-AgNP (blueberry), Lg-AgNP (lingonberry), and Sb-AgNP (sea buckthorn); BbAE + AgNO₃, LgAE + AgNO₃, and SbAE + AgNO₃ represent the mixtures of each berry extract with 1 mM AgNO₃. The mixture of berry aqueous extracts (BbAE, LgAE, SbAE) with 1 mM AgNO₃ in the same ratio as used for Bb-AgNP synthesis, and chemically synthesized silver nanoparticles (chem-AgNP). There were two narrowed peaks in the both Lg-AgNP and Sb-AgNP UV-visible spectra due to excess berry extracts. The maximum absorbance for AgNPs, depending on the particle properties, was around 390-423 nm of wavelength [18]. Finally, chemically synthesized silver nanoparticle showed maximum adsorption at around 440 nm (Fig. 1). The appearance of a peak in the chem-AgNP was single and very broadened, indicating that the chem-AgNPs were polydispersed and small sized nanoparticles [23].

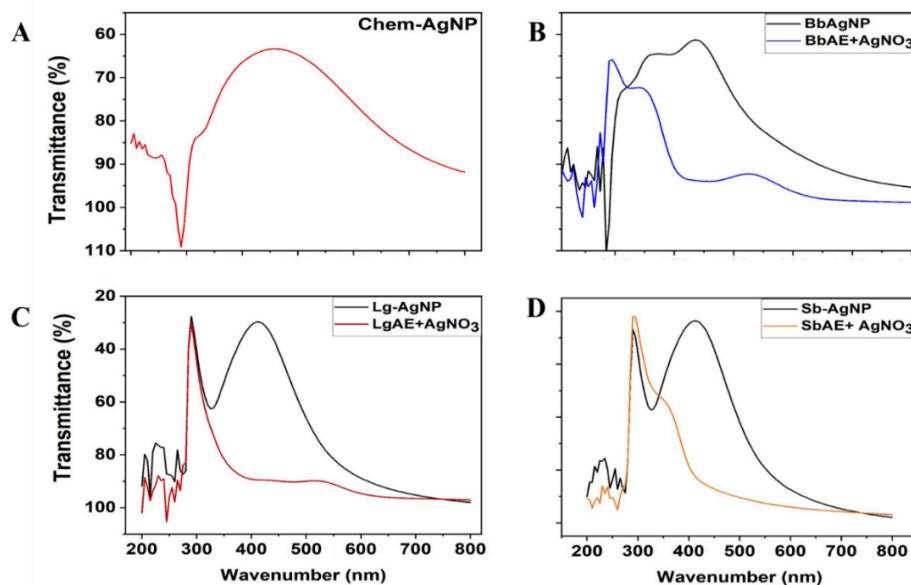


Fig. 1. UV-visible spectra of silver nanoparticles synthesized from blueberry (Bb-AgNP), lingonberry (Lg-AgNP), and sea buckthorn (Sb-AgNP) extracts, along with their corresponding extract- AgNO_3 mixtures and chemically synthesized AgNPs

The maximum absorption peaks of the aqueous extract from the berries and 1 mM AgNO_3 mixture were observed at around 295 nm. In contrast, the maximum absorption peaks of the synthesized silver nanoparticles ranged around 410–445 nm, demonstrating the formation of AgNP (Fig. 1 and Table 2) [18]. The peak of the Bb-AgNP was broadened and there was a bathochromic shift (red shift) with a hyperchromic effect. The broadened peak indicated polydispersed AgNP [23]. The appearance of a single peak in the AgNP spectrum proposed that the formatted AgNPs had small-sized and spherical shape of [1, 7] nanoparticles which was further validated using scanning electron microscopy.

Table 2. Maximum adsorption wave numbers of the berry silver nanoparticles, the mixtures of the berry AE and 1 mM AgNO_3 and chem-AgNP

Berries	λ_{max} , nm	
	Berry AE + AgNO_3	Berry-AgNP
Blueberry	295	445
Lingonberry	290	410
Sea buckthorn	295	410
Chem-AgNP		440

FTIR spectroscopy: FTIR analysis was performed on the synthesized AgNPs to identify the possible reducing biomolecules within the berry extracts. The FTIR spectra are shown in Fig. 2.

The FTIR spectrum of BbAE showed absorption peaks at 3307.03, 2914.9, 1717.01, 1622.03, 1416.22, 1231.53, 1041.55, and 593.01 cm^{-1} , indicating the presence of the following main compounds in the berry extract: primary amines, alcohols, phenolic compounds, flavonoids, and organic acids. However, the FTIR spectrum of Bb-AgNPs showed fewer peaks at 3373.72, 1641.60, 1056.09, and 550.40 cm^{-1} .

The peaks at 1717.01 cm^{-1} , 1416.22 cm^{-1} , and 1086.80 cm^{-1} , related to the stretching vibrations of $-\text{C}=\text{O}$ and $\text{C}-\text{C}$ bonds in alcohols, carboxylic acids, polyphenolic compounds, and phenols, were not present in the spectrum of the Bb-AgNP. Therefore, alcohols, carboxylic acids, and phenolic compounds in BbAE played a major role in the formation of silver nanoparticles. The peak at 1622.03 cm^{-1} , related to the stretching vibration of the $\text{C}=\text{O}$ bond of the carboxyl group, $\text{C}=\text{C}$ stretching in aromatic compounds, and $\text{N}-\text{H}$ in primary amines [23], slightly shifted to 1641.60 cm^{-1} , indicating that the carboxyl group and primary amines contributed to the formation of Bb-AgNPs. Furthermore, the peak at 1041.55 cm^{-1} , related to $-\text{C}-\text{O}$ stretching vibrations of alcoholic groups [7] shifted to 1056.09 cm^{-1} , suggesting that alcoholic groups also played a role in the formation of Bb-AgNPs.

The FTIR spectrum of LgAE showed absorption peaks at 3314.63, 2926.81, 1710.07, 1622.03, 1206.17, 1038.27, and 592.20 cm^{-1} , indicating the presence of the following main compounds in the berry extract: alcohols, phenolic compounds, flavonoids, and organic acids. All of these peaks were not present in the FTIR spectrum of Lg-AgNPs, except for one peak at 3291.82 cm^{-1} , which is related to $\text{O}-\text{H}$ group stretching vibrations from water. However, the FTIR spectrum of Lg-AgNPs showed fewer peaks at 3291.82, 1631.03, and 440.11 cm^{-1} . This suggests that alcohols, carboxylic acids, and phenolic compounds in LgAE played a major role in the formation of silver nanoparticles. The peak at 1621.03 cm^{-1} , related to the stretching vibration of the $\text{C}=\text{O}$ bond in carboxyl groups [24], $\text{C}=\text{C}$ stretching in aromatic compounds, and $\text{N}-\text{H}$ in primary amines [7], slightly shifted to 1631.03 cm^{-1} , indicating that carboxyl groups and primary amines contributed to the formation of Lg-AgNPs.

Additionally, the sharp band at 440.11 cm^{-1} in the Lg-AgNP spectrum suggested the presence of an Ag-O bond.

There are secondary metabolites responsible for the antioxidant activity of blueberry extract. These are flavonoids: quercetin and kaempferol; phenolic acid: chlorogenic acid; primary anthocyanins: delphinidin-3-galactoside, cyanidin-3-galactoside, petunidin-3-galactoside, peonidin-3-galactoside, malvidin-3-galactoside, proanthocyanidins: catechin and epicatechin units.

The FTIR spectrum of SbAE showed absorption peaks at 3329.84 , 2919.2 , 1721.83 , 1596.01 , 1421.10 , 1215.78 , 1086.80 , 615.01 and 516.15 cm^{-1} , indicating the presence of the following main compounds in the berry extract: primary amines, alcohols, phenolic compounds, flavonoids, and organic acids. However, the FTIR spectrum of Bb-AgNP showed fewer peaks at 3299.42 , 1634.03 and 630.22 cm^{-1} . The peaks at 1717.01 cm^{-1} , 1416.22 cm^{-1} , 1215.78 cm^{-1} and 1086.80 cm^{-1} were related to stretching vibrations -C=O and C-C bonds in alcohols, carboxylic acids, polyphenolic compounds pheols [25] and C-H deformation vibration and N-H primary amines in aromatic ring; those peaks were no longer present. Therefore, alcohols, carboxylic acids and phenolic compounds and primary amine functional groups in SbAE played a major role in formation of silver nanoparticles. The peak at 1596.01 cm^{-1} in the spectrum of the SbAE, related to stretching vibration of the C-O bond of carboxyl group, C=C stretching in aromatic compounds and N-H primary amines [26], slightly shifted to 1634.03 cm^{-1} ; this indicated the carboxyl group and primary amines played role the formation of the Sb-AgNP. The absence of those peaks in the berry-AgNPs spectrum and modification of the peaks indicate that those secondary

metabolites likely play a part in capping and reducing silver to AgNPs in the process of nanoparticle synthesis [27]. Biomolecules present in plant extracts serve crucial roles in both the capping and stabilization of the synthesized nanoparticles. Phenols (OH group) and proteins (carbonyl group) exhibit specific attractions to silver and other metals, forming a protective layer around the nanoparticles, thereby acting as a capping agent [4]. Additionally, amines and alcohols play a role in preventing the nanoparticles from agglomeration during their synthesis. Meanwhile, all the IR spectrum of berry-AgNPs displayed sharp broadened peaks in the region between 500 cm^{-1} to 400 cm^{-1} , which was attributed to the metal-oxygen bonds [24]. The FTIR spectra clearly indicate that the phytochemicals are well-coated on the AgNPs, playing a key role in their formation and stability [28]. However, chemically synthesized nanoparticles showed major FTIR peaks at 1579.88 and 1407.08 cm^{-1} . The bands at 1579 and 1407 cm^{-1} correspond to the symmetric and asymmetric stretching of COO^- groups present in the citrate ions used for reduction [29].

Zeta potential analysis: Zeta potential explains the stability, dispersion and surface charge of the nanoparticles. A zeta potential greater than $+30\text{ mV}$ or less than -30 mV indicates high stability of nanoparticles in dry powder form [30]. The high negative value produces repulsion between similarly charged particles in suspension, therefore resisting aggregation. Several studies that were done on silver nanoparticle synthesis with berry extracts such as sea buckthorn berries, rowan berries, hawthorn berries resulted in zeta potential of -26.3 mV , -28.8 mV , -38.2 mV respectively [3, 7, 9]. Our results showed that zeta potential of the synthesized Bb-AgNP, Lg-AgNP, Sb-AgNP had an average zeta potential of $-43.6 \pm 0.11\text{ mV}$,

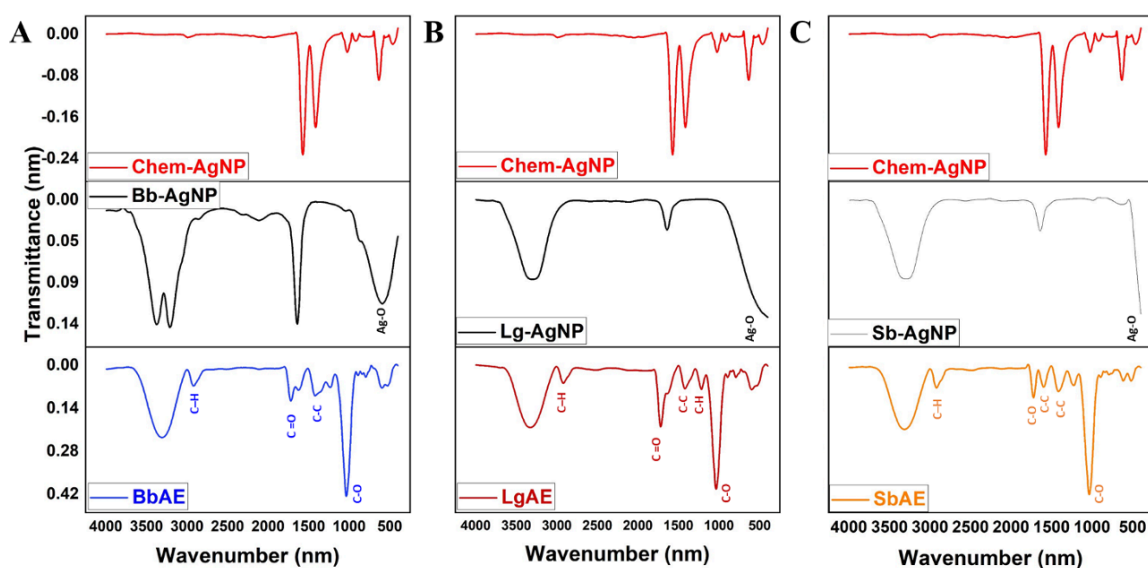


Fig. 2. FTIR spectra for the synthesized silver nanoparticles. A. BbAE and Bb-AgNP and chem-AgNP, B. LgAE and Lg-AgNP and chem-AgNP, C. SbAE and Sb-AgNP and chem-AgNP

-51.1 ± 1.91 mV, -42.8 ± 0.8 mV. The zeta potential of Lg-AgNP exhibited a higher average value compared to the Bb-AgNP and Sb-AgNP; this may be due to the presence of different phytochemicals in each sample that reduced and capped silver nanoparticles. Results showed that synthesized silver nanoparticles were quite stable with lower negative values.

Fig. 3 shows the variation in zeta potential (ZP) of the green-synthesized silver nanoparticles Bb-AgNP, Lg-AgNP, and Sb-AgNP across a pH range of 3-11. For Bb-AgNPs and Lg-AgNPs, relatively high ZP values (around -30 to -35 mV) were recorded under acidic conditions (pH 3-4), followed by a sharp decrease near pH 5, reaching approximately -70 to -75 mV, indicating maximum colloidal stability due to enhanced electrostatic repulsion. As pH increased toward the alkaline range (pH 7-11), the ZP gradually rose to around -40 mV, suggesting partial neutralization of surface charge but still maintaining sufficient repulsion to prevent aggregation. In contrast, Sb-AgNPs showed less pronounced variation, with ZP values ranging from -25 mV at acidic pH to -40 mV at alkaline pH, implying

relatively stable colloidal behavior throughout the pH range. Overall, pH influenced the surface charge of the nanoparticles, with optimal stability observed around pH 5 (Fig. 3).

The stability of AgNPs, as indicated by their zeta potential, is significantly influenced by the pH of the medium. All three types of AgNPs show a decrease in stability around pH 5-6, suggesting aggregation tendencies at this pH range.

The stability at acidic and alkaline conditions suggests that surface charge plays a crucial role in maintaining colloidal stability. Notably, the different green synthesis methods result in distinct ZP patterns, indicating that the synthesis method and the capping agents used significantly impact the stability of AgNPs in various pH conditions.

Fig. 4 illustrates the variation in electrical conductivity of the synthesized silver nanoparticles (AgNPs) at different pH levels. For both Bb-AgNP and Lg-AgNP, conductivity shows a steady and nearly linear increase from approximately 0.1 mS/m at acidic pH (3-4) to about 0.7 mS/m at alkaline pH (10-11).

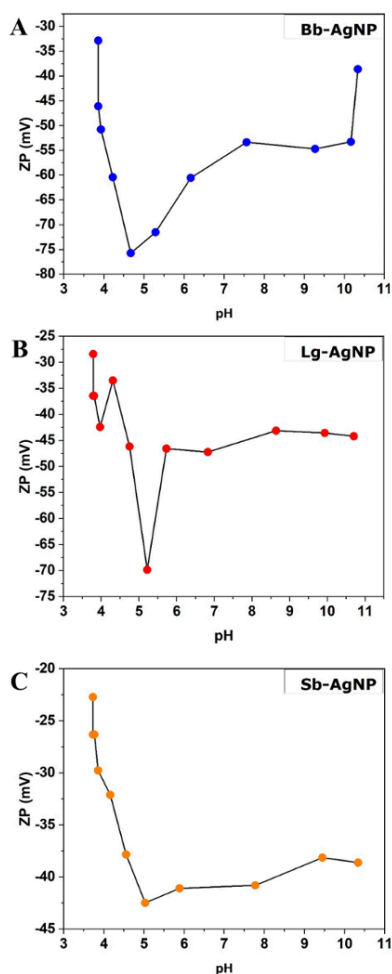


Fig. 3. Zeta potential for the synthesized silver nanoparticles at different pH levels. A. Bb-AgNP, B. Lg-AgNP, C. Sb-AgNP

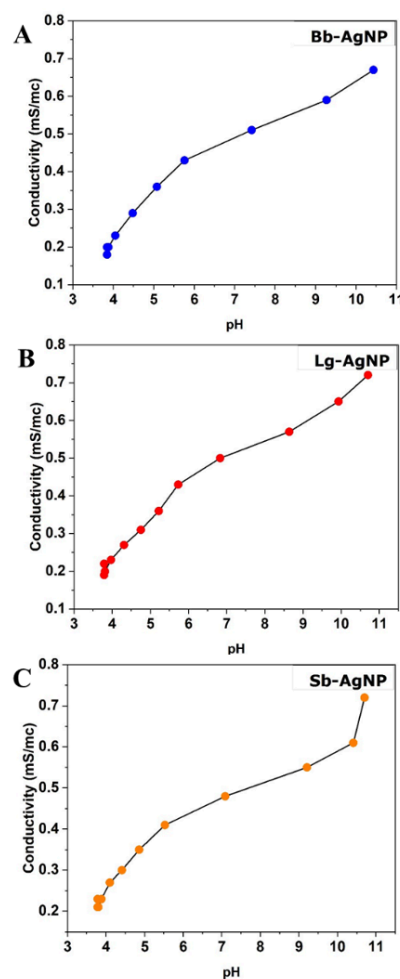


Fig. 4. Conductivity for the synthesized silver nanoparticles at different pH levels. A. Bb-AgNP, B. Lg-AgNP, C. Sb-AgNP

This progressive rise suggests enhanced ion mobility and particle dispersion under basic conditions, likely due to increased surface charge and reduced particle aggregation. In contrast, Sb-AgNP exhibits a similar increasing trend, although with slightly lower overall conductivity values, indicating differences in surface chemistry or capping efficiency among the berry-derived nanoparticles. The highest conductivity values recorded at alkaline pH confirm improved colloidal stability and electrostatic repulsion between particles under these conditions (Fig. 4).

The conductivity of all three AgNP types shows a positive correlation with increasing pH, indicating that higher alkalinity enhances the ionic mobility or charge distribution on the nanoparticle surface. This may be attributed to the deprotonation of surface functional groups, increasing the availability of free ions and thus enhancing conductivity. Among the three types, Lg-AgNP exhibits the highest conductivity at alkaline pH, while Sb-AgNP shows a slower increase compared to the other two. These differences are likely due to variations in the green synthesis methods and the resulting surface chemistry of the nanoparticles.

Morphology and size histograms of the AgNPs from the berry extracts:

SEM images and particle size distributions of silver nanoparticles synthesized using Blueberry (Bb-AgNPs), Lingonberry (Lg-AgNPs), and Sea buckthorn berry (Sb-AgNPs) extracts are shown, with distributions fitted to a Gaussian (log-normal) function based on 116, 182, and 173 particles, respectively (Fig. 5). The particle sizes were analyzed by using SEM and images are displayed in Fig. 5.

The images show that nanoparticles were in spherical morphology and nanoparticles were homogeneously distributed, and their size was non-uniform.

The size of the synthesized Bb-AgNPs ranged from 17.29 to 55.74 nm. The Bb-AgNPs exhibited an average size of 32.36 ± 1.24 nm (Fig. 5), which is relatively typical compared to silver nanoparticles reported in other studies [7, 27]. For example, in 2014, Mallikarjuna *et al.* [2] synthesized AgNPs using Bb extract, revealing AgNP sizes ranging from 50 to 150 nm with spherical and triangular shapes. The variation in nanoparticle size may be due to differences in the silver nanoparticle synthesis methods; they did not apply heat during the stirring process and stirred for a longer duration.

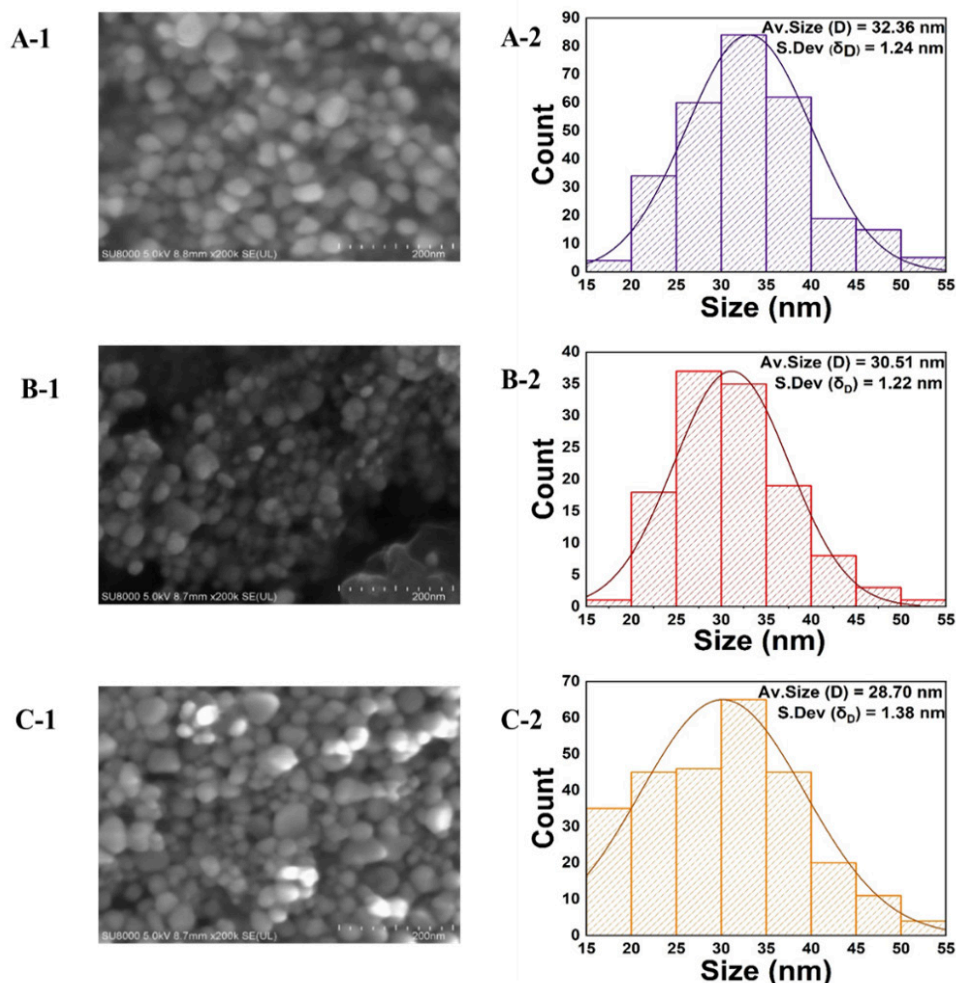


Fig. 5. SEM images and particle size distributions of green-synthesized silver nanoparticles: (A-1, A-2) Bb-AgNPs (blueberry), (B-1, B-2) Lg-AgNPs (lingonberry), and (C-1, C-2) Sb-AgNPs (sea buckthorn). Particle size distributions were fitted with a Gaussian (log-normal) function ($n = 116, 182, \text{ and } 173$, respectively).

The size of the synthesized Lg-AgNPs in our study ranged from 16.24 to 59.56 nm. The Lg-AgNPs exhibited an average size of 36.56 ± 7.86 nm, which was larger than that of other silver nanoparticles (Fig. 5). In 2023, Rizwana *et al.* synthesized AgNPs using LgAE [8], achieving a particle size of 5-30 nm, smaller than our findings.

The size of the synthesized Sb-AgNPs ranged from 10.58 to 56.98 nm. The Sb-AgNPs exhibited an average size of 28.70 ± 1.38 nm, representing the smallest size compared to the silver nanoparticles synthesized in this study (Fig. 5). Nanoparticles with reduced dimensions had a high surface-to-volume ratio, suggesting significant potential for surface reaction-based applications, such as antimicrobial activity.

The polydispersity index (PDI) values of the synthesized silver nanoparticles were remarkably low: Bb-AgNP: 0.0015, Lg-AgNP: 0.0016, and Sb-AgNP: 0.0023. These values were all well below 0.1, indicating an extremely narrow size distribution and thus high monodispersity of the particles. Lg-AgNPs showed the highest antibacterial and antioxidant activity and also had one of the lowest PDI values. This supports the idea that monodispersity enhances bioactivity, possibly by promoting uniform cellular uptake and interaction with microbial membranes [31]. However, since all three AgNP formulations exhibited extremely low PDI, any observed differences in activity were more likely due to factors such as particle size, surface chemistry, and bioactive compounds from the plant extracts, rather than polydispersity alone.

X-ray diffraction: The purity, size, and crystalline structure of the synthesized berries-AgNPs were analyzed using X-ray diffraction (XRD) (Fig. 6).

For Bb-AgNPs, four distinct peaks at 38.16° , 44.26° , 64.56° , and 77.44° corresponded to the (111), (200),

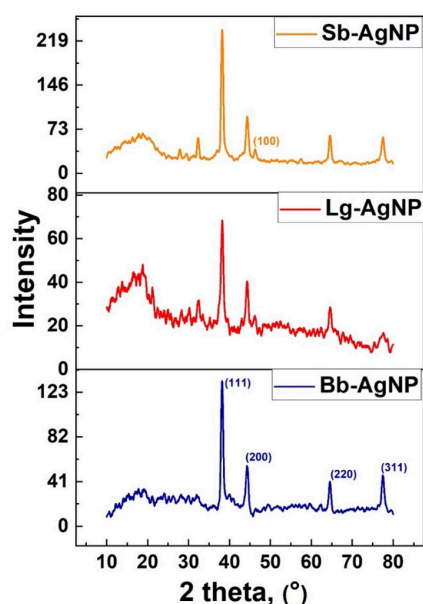


Fig. 6. XRD patterns of green-synthesized silver nanoparticles (AgNPs) obtained from three Mongolian wild berry extracts

(220), and (311) planes of cubic silver (JCPDS files 04-0783 and 41-1402), confirming their crystalline nature. The most intense peak appeared at $2\theta = 38.16^\circ$, and the crystallinity index (26.46%) indicated a moderate level of crystallinity, suggesting a balance between crystalline and amorphous phases.

For Lg-AgNPs, peaks similar to Bb-AgNPs were observed at 38.22° , 44.28° , 64.54° , and 77.56° , corresponding to the same planes and confirming their crystalline structure. Additional peaks at 32.52° and 18.78° also appeared, likely from organic compounds in the lingonberry extract. The strongest diffraction peak occurred at $2\theta = 38.22^\circ$, and the crystallinity index (17.63%) suggested a predominantly amorphous material.

For Sb-AgNPs, five sharp peaks at 38.2° , 44.32° , 46.06° , 64.58° , and 77.52° were assigned to the (111), (100), (200), (220), and (311) planes of cubic silver, confirming crystallinity.

Additional peaks at 27.86° , 29.40° , 32.34° , and 18.72° may result from organic compounds in the sea buckthorn extract. The most intense peak appeared at $2\theta = 38.2^\circ$, and the crystallinity index (38.54%) indicated a moderate crystalline phase.

Antioxidant assays of berry aqueous extracts (AEs) and berry-derived silver nanoparticles (AgNPs):

As an extract from important food resource and their silver nanoparticles (AE berries and FrAgNP) were investigated for the radical scavenging capacity of DPPH $^{\cdot}$ and ABTS $^{2+}$ methods. In all tests ascorbic acid (vitamin C) and rutin were used as standard compounds. Results are shown in Fig. 7 and Table 3.

The DPPH $^{\cdot}$ test revealed that LgAE exhibited the highest activity compared to the other berry extracts and even exhibited higher than positive standards for antioxidant activity. The chem-AgNP, however, showed no activity. Consistent with the present study, previous research has demonstrated dose-dependent free radical scavenging activity for lingonberry extracts [8]. For the synthesized silver nanoparticles, BbAE did not show antioxidant activity, whereas Bb-AgNP exhibited greater activity. However, Lg-AgNP displayed slightly reduced activity compared to its extract.

Sea buckthorn berry extract showed antioxidant activity, but its silver nanoparticles exhibited weakened activity. In contrast, an earlier study reported that Sb-AgNP displayed dose-dependent antioxidant activity in DPPH free radical scavenging assay [9].

The ABTS $^{2+}$ test revealed that LgAE exhibited the highest activity compared to the other fruit extracts and even exhibited higher than positive standards. The chem-AgNP, however, showed no activity. For the synthesized silver nanoparticles, BbAE did not show antioxidant activity, whereas Bb-AgNP exhibited greater activity. However, while LgAE was highly active, Lg-AgNP demonstrated even higher activity. SbAE did not show antioxidant activity, and neither did its silver nanoparticles.

Table 3. IC₅₀ values of the the berry extracts, synthesized AgNPs and chem-AgNP

Sample	Average size, nm	Antioxidant activities, IC ₅₀ µg/mL	
		DPPH [•]	ABTS ^{•+}
Vitamin C		106.67 ± 2.51	320.405 ± 2.43
Rutin		49.57 ± 0.71	248.59 ± 4.05
Chem-AgNP		-	2426 ± 53.39
BbAE		217.91 ± 17.03	421.10 ± 16.33
Bb-AgNP	32.36 ± 1.23	179.3 ± 7.23	28.72 ± 0.06
LgAE		34.00 ± 2.71	143.73 ± 8.96
Lg-AgNP	36.56 ± 7.86	39.66 ± 1.79	11.28 ± 1.38
SbAE		103.64 ± 7.29	942.60 ± 83.33
Sb-AgNP	28.70 ± 1.38	173.00 ± 13.31	2280.92 ± 90.33

↑ - increased

↓ - decreased

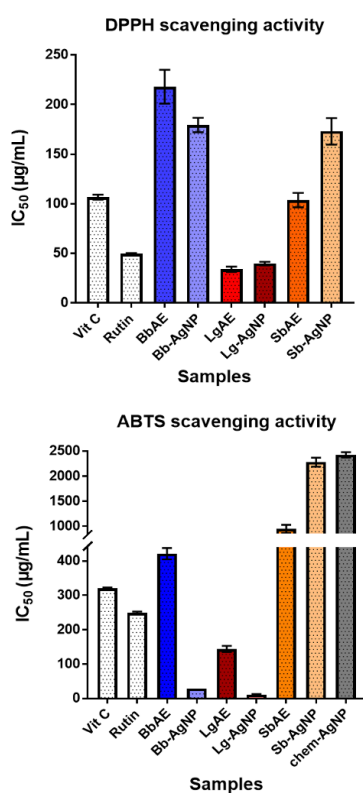


Fig. 7. Antioxidant activities of berry extracts (BbAE, LgAE, SbAE), their green-synthesized AgNPs (Bb-AgNPs, Lg-AgNPs, Sb-AgNPs), and chem-AgNPs, measured by (A) DPPH[•] and (B) ABTS^{•+} scavenging assays. Results are shown as mean ± SD of three independent experiments ($P < 0.05$).

Additionally, LgAE and Lg-AgNP demonstrated the strongest activity compared to other samples, as well as the positive and negative standards in both assays. Consistent with the present study, previous research has shown that LgAE and Lg-AgNP possess potent antioxidant properties [8].

The observed differences in antioxidant activity between the berry aqueous extracts and their corresponding silver nanoparticles (AgNPs) can be attributed to the distinct phytochemical compositions and interactions

between the plant-derived phytochemicals and silver ions during nanoparticle synthesis.

In the case of blueberry (Bb) and lingonberry (Lg), the green synthesized AgNPs exhibited higher antioxidant activity than the crude extracts.

The antioxidant activity of BbAE is primary attributed to its rich content of flavonoids: quercetin, kaempferol [32], phenolic acids including chlorogenic acid, and anthocyanins such as delphinidin-3-galactoside, cyanidin-3-galactoside, petunidin-3-galactoside, peonidin-3-galactoside, malvidin-3-galactoside [33]. Additionally, proanthocyanidins composed of catechin and epicatechin units contribute significantly to its antioxidant activity [34]. Among these, gallic acid and proanthocyanidins have been shown to play a crucial role in the green synthesis of the silver nanoparticles, acting as reducing agent [35, 36], capping the surface, preventing aggregation and controlling particle size [37].

Similarly, lingonberry extract contains comparable phytochemicals but differs in the concentration and identity of key compounds. Major anthocyanins in lingonberry include cyanidin-3-glucoside and cyanidin-3-arabinoside [38], alongside phenolic acids such as caffeic acid and ferulic acid [39] and triterpenoids like ursolic acid [40]. Among these, anthocyanins [41] and phenolic acids [42] have demonstrated effective reducing and capping capabilities in AgNP synthesis. The resulting Lg-AgNPs exhibit enhanced antioxidant activity. This enhancement may result from the synergistic interaction between residual polyphenolic compounds capping the nanoparticles and the increased surface reactivity of the nanoscale silver [31, 35]. Moreover, it could be attributed to Lg-AgNPs small particle size, low polydispersity index (PDI), and improved dispersion and reactivity toward radical species [43].

In contrast, in the case of sea buckthorn, the aqueous extract showed significantly higher antioxidant activity than its respective nanoparticles. Sea buckthorn berries contain a unique phytochemical profile, including high levels of isorhamnetin glycosides (isorhamnetin-3-O-

glucoside and isorhamnetin-3-O-rutinoside), ascorbic acid, ellagic acid, and specific proanthocyanidins [44]. These compounds collectively contribute to the berry extract's potent antioxidant activity, setting it apart from lingonberry and blueberry extracts. These distinctive phytochemicals contribute significantly to the antioxidant properties of sea buckthorn [44]. Although green-synthesized silver nanoparticles (AgNPs) often exhibit enhanced antioxidant activity compared to their source extracts, the opposite can occur, observed in our experimental results for sea buckthorn, where the extract's antioxidant potential was significantly higher than that of the Sb-AgNP. This can occur because the silver nanoparticle synthesizing process may consume a portion of the most potent antioxidants, especially ascorbic acid and phenolic acids, in the reduction of silver ions. Once oxidized, these molecules may lose their antioxidant functionality [35].

Moreover, not all antioxidants from the extract are successfully adsorbed onto the surface of AgNPs, which means a significant portion of active compounds may be lost during nanoparticle formation.

Therefore, the variation in antioxidant behavior among the different berry-derived AgNPs is likely influenced by both phytochemical composition and physicochemical properties of the resulting nanoparticles such as size, PDI, and surface chemistry [31].

Antibacterial activity: *In vitro* evaluation of antimicrobial properties of green synthesized silver nanoparticles against typical pathogens i.e., *S. aureus*, *P. aeruginosa*, *E. coli*, *E. faecalis*, *B. subtilis*, and *M.*

luteus was realized by the agar disk diffusion method. The results were shown in Fig. 8. The microorganism inhibition process follows a specific mechanism.

As the silver nanoparticles (AgNPs) attach to the negatively charged surface of the bacterial cell, they alter the chemical composition and structural integrity of the cell wall and plasmalemma, disrupting functions such as permeability, electron transport, and respiration. The silver NPs penetrate the bacterial cells, causing further damage.

Once inside, the particles interact with the DNA, phosphorous compounds, and various proteins of the cell. The release of silver ions from the AgNPs generates reactive oxygen species (ROS), contributing to cellular damage [30]. Among the synthesized silver nanoparticles, Lg-AgNPs exhibited the largest inhibition zones against *E. coli*, *E. faecalis*, indicating the strongest antibacterial efficacy. A large inhibition zone typically indicates that the nanoparticles have a higher potential to disrupt bacterial cell membranes, generate reactive oxygen species (ROS), or interact with intracellular components [45]. These findings support the high antibacterial potential of Lg-AgNPs and their efficient interaction with microbial cells.

Bb-AgNP exhibited the largest inhibition zone against *S. aureus* and showed comparable efficacy to Lg-AgNPs against *P. aeruginosa* and *B. subtilis*, indicating that the bioactive compounds present in blueberry extract may enhance the nanoparticles' capping and stabilization, contributing to their antibacterial activity. Furthermore, Bb-AgNPs exhibited significantly larger inhibition zones

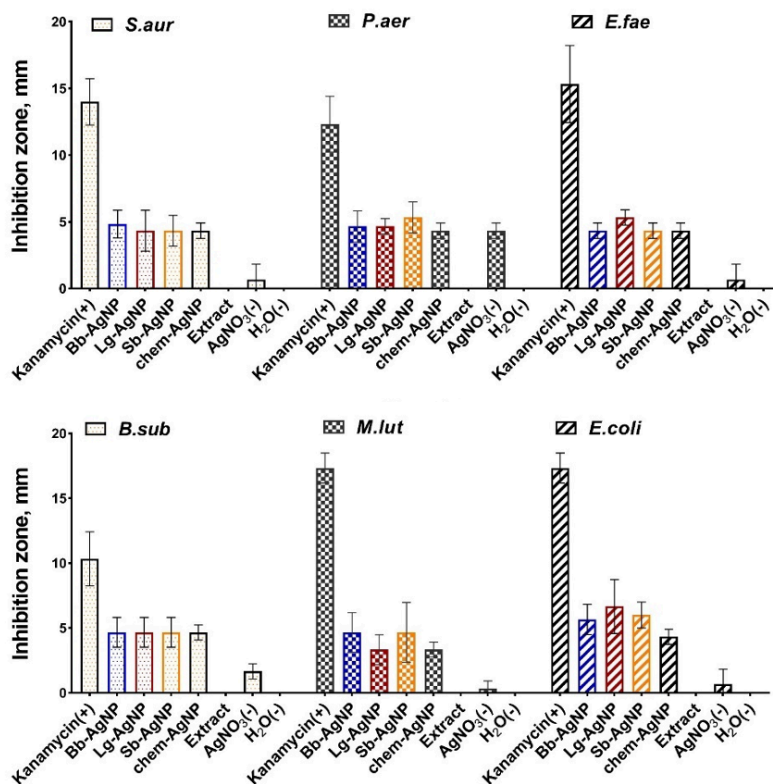


Fig. 8. Diameters of the inhibition zone for the green-synthesized AgNPs from berry extracts against six bacterial strains

compared to distilled water, chemically synthesized AgNPs (chem-AgNPs), and 1 mM AgNO₃, suggesting the potential advantages of plant-mediated synthesis in improving AgNPs' antibacterial efficacy. The Sb-AgNPs showed the largest inhibition zone for the *E. faecalis* among the berry-derived silver nanoparticles but showed comparatively lower antibacterial activity against all other tested bacterial strains. This reduced efficacy may be attributed to factors such as the lower bioavailability of active compounds in the sea buckthorn extract or variations in nanoparticle size, shape, and surface characteristics affecting their interaction with bacterial cells [35].

No inhibition was observed with distilled water and berry extracts, while kanamycin exhibited the strongest inhibition, indicating that the bacterial strains used were highly susceptible to the antibiotic. This highlights the comparative effectiveness of green-synthesized AgNPs as promising antimicrobial agents. These results indicate that monodispersity (uniform particle size) in AgNPs can enhance bioactivity, likely by promoting more uniform interactions with bacterial cell membranes. Further optimization of nanoparticle synthesis may also improve antibacterial activity by controlling particle size and surface characteristics.

CONCLUSION

We have successfully synthesized silver nanoparticles from three different Mongolian wild berry extracts, including blueberry, lingonberry, and sea buckthorn, using a non-toxic, eco-friendly, and cost-effective method. The SbAE produced spherical and smaller-sized AgNPs covered by anion, comparable to those from other berry extracts, while LgAE produced spherical and larger-sized AgNPs covered by anion. When the antioxidant activities of the berry extracts were evaluated as two different antioxidant agents, lingonberry and its silver nanoparticle showed excellent results. But the SbAE revealed poor inhibition activities for both assays. Additionally, AgNP synthesized from LgAE were found to be superior, as they demonstrated high antioxidant activity. The AgNP synthesized from BbAE were found to have better antioxidant activity than its extract. The AgNP synthesized from SbAE was found to have weaker antioxidant activity than its extract. The AgNPs synthesized from LgAE exhibited stronger antibacterial activity than the other synthesized silver nanoparticles. These results reveal that both LgAE and Lg-AgNPs could be promising candidates for antioxidant food supplements, and that Lg-AgNPs exhibit antibacterial activity.

AUTHOR CONTRIBUTIONS

BTs: designed the research, analyzed the data, wrote the manuscript draft; TsTs and NO: performed the experiments; ST: analyzed the data and SO: revised the manuscript. All authors approved the final version of the manuscript.

CONFLICT OF INTEREST

The authors declare no conflict of interest.

ACKNOWLEDGMENTS

The authors would like to acknowledge their respective affiliated institutions and university for their support and facilities. Especially, we acknowledge the Laboratory of Instrumental Analyses for FT-IR, and we also thank Prof. Altan Bolag from Inner Mongolia Normal University, China, for the SEM analysis.

FUNDING

This research work was supported by the major direction research of Institute of Chemistry and Chemical Technology, MAS entitled "Technology development for liver protecting agent using medicinal plants". This work sponsored by post-doctoral grant from the Ministry of Education and Science of Mongolia (STF-2023/274, 2023-2025) titled Derivation of biological active silver nanoparticles (AgNP) by green synthesis using the aqueous extract of *Dracocephalum foetidum*.

ABBREVIATIONS

AgNP-silver nanoparticle; BbAE-blueberry aqueous extract; Berry AE-berry aqueous extract; Bb-AgNP-blueberry silver nanoparticle; LgAE-lingonberry aqueous extract; Lg-AgNP-lingonberry silver nanoparticle; SbAE-sea buckthorn berry aqueous extract; Sb-AgNP-sea buckthorn silver nanoparticle; UV-ultraviolet; FTIR-fourier transform infrared spectroscopy; SEM-scanning electron microscopy; XRD-X-ray diffraction; DPPH-2,2-diphenyl-1-picrylhydrazyl; ABTS-2,2'-azinobis(3-ethylbenzothiazoline-6-sulfonate) radical cation; TPTZ - 2,4,6-tris(2-pyridyl)-s-triazine; IC₅₀-inhibition concentration at 50%.

REFERENCES

- Li K., C Ma., Jian T., Sun H., Wang L., et al. (2017) Making good use of the byproducts of cultivation: green synthesis and antibacterial effects of silver nanoparticles using the leaf extract of blueberry. *J. Food Sci. Technol.*, **54**, 3569-3576. <https://doi.org/10.1007/s13197-017-2815-1>
- Nadagouda M.N., Iyanna N., Lalley J., Han C., Dionysiou D.D., et al. (2014) Synthesis of silver and gold nanoparticles using antioxidants from blackberry, blueberry, pomegranate, and turmeric extracts. *ACS Sustain. Chem. Eng.*, **2**, 1717-1723. <https://doi.org/10.1021/sc500237k>
- Długosz O., Chwastowski J., Banach M. (2020) Hawthorn berries extract for the green synthesis of copper and silver nanoparticles. *Chem. Papers*, **74**, 239-252. <https://doi.org/10.1007/s11696-019-00873-z>
- Rizwana H., Alwhibi M.S., Al-Judaie R.A., Aldehaish H.A., Alsaggabi N.S. (2022) Sunlight-mediated green synthesis of silver nanoparticles using the berries of *ribes rubrum* (red currants):

- characterisation and evaluation of their antifungal and antibacterial activities. *Molecules*, **27**, 2186. <https://doi.org/10.3390/molecules27072186>
5. Joshi N., Jain N., Pathak A., Singh J., Prasad R., et al. (2018) Biosynthesis of silver nanoparticles using *Carissa carandas* berries and its potential antibacterial activities. *J. Solgel Sci. Technol.*, **86**, 682-689. <https://doi.org/10.1007/s10971-018-4666-2>
 6. Amin M., Anwar F., Janjua M.R.S.A., Iqbal M.A., Rashid U. (2012) Green synthesis of silver nanoparticles through reduction with *Solanum xanthocarpum* L. berry extract: Characterization, antimicrobial and urease inhibitory activities against *Helicobacter pylori*. *Int. J. Mol. Sci.*, **13**, 9923-9941. <https://doi.org/10.3390/ijms13089923>
 7. Singh P., Mijakovic I. (2022) Rowan Berries: A potential source for green synthesis of extremely monodisperse gold and silver nanoparticles and their antimicrobial property. *Pharmaceutics*, **14**, 82. <https://doi.org/10.3390/pharmaceutics14010082>
 8. Rizwana H., Khan M., Aldehaish H.A., Adil S.F., Shaik M.R., et al. (2023) Green biosynthesis of silver nanoparticles using *Vaccinium oxycoccos* (cranberry) extract and evaluation of their biomedical potential. *Crystals*, **13**, 294. <https://doi.org/10.3390/cryst13020294>
 9. Wei S., Wang Y., Tang Z., Hu J., Su R., et al. (2020) A size-controlled green synthesis of silver nanoparticles by using the berry extract of Sea Buckthorn and their biological activities. *New J. Chem.*, **44**, 9304-9312. <https://doi.org/10.1039/d0nj01335h>
 10. Nemzer B.V., Al-Taher F., Yashin A., Revelsky I., Yashin Y. (2022) Cranberry: Chemical composition, antioxidant activity and impact on human health. Overview. *Molecules*, **27**, 1-19. <https://doi.org/10.3390/molecules27051503>
 11. Nemzer B.V., Al-Taher F., Yashin A., Revelsky I., Yashin Y. (2022) Cranberry: Chemical composition, antioxidant activity and impact on human health. Overview. *Molecules*, **27**, 1-19. <https://doi.org/10.3390/molecules27051503>
 12. Ștefănescu B. E., Călinoiu L. F., Ranga F., Fetea F., Mocan A., et al. (2020) Chemical composition and biological activities of the nord-west romanian wild bilberry (*Vaccinium myrtillus* L.) and lingonberry (*Vaccinium vitis-idaea* L.) leaves. *Antioxidants*, **6**, 495. <https://doi.org/10.3390/antiox9060495>
 13. Bouyahya A., Omari N. E., Hachlafi N. E., Jemly M.E., Hakkour M., et al. (2022) Chemical compounds of berry-derived polyphenols and their effects on gut microbiota, inflammation, and cancer. *Molecules*, **27**, 3286. <https://doi.org/10.3390/molecules27103286>
 14. Zenkova M., Pinchykova J., (2019) Chemical composition of sea-buckthorn and highbush blueberry fruits grown in the Republic of Belarus. *J. Food Sc. App. Biotech.*, **2**, 121-129. <https://doi.org/10.30721/fsab2019.V2.I2.59>
 15. Tkacz K., Chmielewska J., Turkiewicz I. P., Nowicka P., Wojdyło A., (2020) Dynamics of changes in organic acids, sugars and phenolic compounds and antioxidant activity of sea buckthorn and sea buckthorn-apple juices during malolactic fermentation. *Food Chem*, **332**, 127382. <https://doi.org/10.1016/J.foodchem.2020.127382>
 16. Zhang A., Deng J., Liu X., He P., He L., et al. (2018) Structure and conformation of α -glucan extracted from *Agaricus blazei* Murill by high-speed shearing homogenization. *Int. J. Biol. Macromol.*, **113**, 558-564. <https://doi.org/10.1016/j.ijbiomac.2018.02.151>
 17. Chung I., Rahuman A.A., Marimuthu S., Kirthi A.V., Anbarasan K., et al. (2017) Green synthesis of copper nanoparticles using eclipta prostrata leaves extract and their antioxidant and cytotoxic activities. *Exp. Ther. Med.*, **14**, 18-24. <https://doi.org/10.3892/etm.2017.4466>
 18. Morais M., Teixeira A.L., Dias F., Machado V., Medeiros R., et al. (2020) Cytotoxic effect of silver nanoparticles synthesized by green methods in cancer. *J. Med. Chem.*, **63**, 14308-14335. <https://doi.org/10.1021/acs.jmedchem.0c01055>
 19. Tsolmon B., Fang Y., Yang T., Guo L., He K., et al. (2021) Structural identification and UPLC-ESI-QTOF-MS² analysis of flavonoids in the aquatic plant *Landoltia punctata* and their *in vitro* and *in vivo* antioxidant activities. *Food Chem.*, **343**, 128392. <https://doi.org/10.1016/j.foodchem.2020.128392>
 20. De Souza V.R., Pereira P.A.P., Da Silva T.L.T., De Oliveira Lima L.C., Pio R., et al. (2014) Determination of the bioactive compounds, antioxidant activity and chemical composition of Brazilian blackberry, red raspberry, strawberry, blueberry and sweet cherry fruits. *Food Chem.*, **156**, 362-368. <https://doi.org/10.1016/j.foodchem.2014.01.125>
 21. Klavins L., Klavina L., Huna A., and Klavins M. (2015) Polyphenols, carbohydrates and lipids in berries of *Vaccinium* species. *Environ. Exp. Biol.*, **13**, 147-158.
 22. Drózdź P., Šežienė V., and Pyrzyńska K., (2017) Phytochemical properties and antioxidant activities of extracts from wild blueberries and lingonberries. *Plant Foods Hum. Nutr.*, **72**, 360. <https://doi.org/10.1007/S11130-017-0640-3>
 23. Pathania D., Pathania D., Kumar S., Thakur P., Chaudhary V., et al. (2022) Essential oil-mediated biocompatible magnesium nanoparticles with enhanced antibacterial, antifungal, and photocatalytic efficacies. *Sci. Rep.*, **12**, 1-13. <https://doi.org/10.1038/s41598-022-14984-3>
 24. Flieger J., Franus W., Panek R., Szymańska-Chargot M., Flieger W., et al. (2021) Green synthesis of silver nanoparticles using natural extracts with proven antioxidant activity. *Molecules*, **26**, 16. <https://doi.org/10.3390/molecules26164986>

25. Sharifi-Rad M., Pohl P., Epifano F., Álvarez-Suarez J.M. (2020) Green synthesis of silver nanoparticles using astragalus tribuloides delille. Root extract: Characterization, antioxidant, antibacterial, and anti-inflammatory activities. *Nanomaterials*, **10**, 1-17. <https://doi.org/10.3390/nano10122383>
26. Dakshayani S.S., Marulasiddeshwara M.B., Sharath Kumar M.N., Ramesh G., Raghavendra Kumar P., et al. (2019) Antimicrobial, anticoagulant and antiplatelet activities of green synthesized silver nanoparticles using Selaginella (Sanjeevini) plant extract. *Elsevier B.V.*, **131**, 787-797. <https://doi.org/10.1016/j.ijbiomac.2019.01.222>
27. Vasyliov G., Vorobyova V., Skiba M., Khrokalo L. (2020) Green synthesis of silver nanoparticles using waste products (apricot and black currant pomace) aqueous extracts and their characterization. *Adv. Mat. Sci. Eng.*, **1**, 11. <https://doi.org/10.1155/2020/4505787>
28. Saif S., Tahir A., Chen Y. (2016) Green synthesis of iron nanoparticles and their environmental applications and implications. *Nanomaterials*, **6**, 209. <https://doi.org/10.3390/nano6110209>
29. Sreelekha E., George B., Shyam A., Sajina N., Mathew B. (2021) A Comparative study on the synthesis, characterization, and antioxidant activity of green and chemically synthesized silver nanoparticles. *Bionanosci.*, **11**, 489-496. <https://doi.org/10.1007/s12668-021-00824-7>
30. Urnukhsaikhan E., Bold B.E., Gunbileg A., Sukhbaatar N., Mishig-Ochir T. (2021) Antibacterial activity and characteristics of silver nanoparticles biosynthesized from *Carduus crispus*. *Sci. Rep.*, **11**, 1-13. <https://doi.org/10.1038/s41598-021-00520-2>
31. Zhang X.F., Liu Z.G., Shen W., Gurunathan S. (2016) Silver nanoparticles: Synthesis, characterization, properties, applications, and therapeutic approaches. *Inter. J. Mol. Sci.*, **17**, 1534. <https://doi.org/10.3390/ijms17091534>
32. Skrovankova S., Sumczynski D., Mlcek J., Jurikova T., Sochor J. (2015) Bioactive compounds and antioxidant activity in different types of berries. *Int. J. Mol. Sci.*, **16**, 24673-24706. <https://doi.org/10.3390/ijms161024673>
33. Chen C.F., Li Y.D., Xu Z. (2010) Chemical principles and bioactivities of blueberry. *Acta Pharmaceutica Sinica*, **45**, 422-429.
34. Huang W-Y., Zhang H-C., Liu W-X., Li C-Y. (2012) Survey of antioxidant capacity and phenolic composition of blueberry, blackberry, and strawberry in Nanjing. *J. Zhejiang Univ-Sci. B*, **13**, 94-102. <https://doi.org/10.1631/jzus.B1100137>
35. Iravani S. (2011) Green synthesis of metal nanoparticles using plants. *Green Chem.*, **13**, 2638-2650. <https://doi.org/10.1039/c1gc15386b>
36. Ahmed S., Ahmad M., Swami B.L., Ikram S. (2016) A review on plants extract mediated synthesis of silver nanoparticles for antimicrobial applications: A green expertise. *J. Adv. Res*, **7**, 17-28. <https://doi.org/10.1016/j.jare.2015.02.007>
37. Muntasir M., Muhib A., Mubassira M., Khanam S., Abeer-Ul-Haque S., et al. (2024) A systematic review on green synthesis of silver nanoparticles, characterization and applications. *World J. Adv. Res. Rev.*, **21**, 1221-1238. <https://doi.org/10.30574/wjarr.2024.21.3.0744>
38. Törrönen R., Järvinen S., Kolehmainen M. (2022) Postprandial glycemic responses to a high-protein dairy snack and energy-enriched berry snacks in older adults. *Clin. Nutr. ESPEN*, **51**, 231-238. <https://doi.org/10.1016/j.clnesp.2022.08.026>
39. Kim J.S. (2018) Antioxidant activities of selected berries and their free, esterified, and insoluble-bound phenolic acid contents. *Prev. Nutr. Food. Sci.*, **23**, 35-45. <https://doi.org/10.3746/pnf.2018.23.1.35>
40. Xu J., Yang H., Nie C., Wang T., Qin X., et al. (2023) Comprehensive phytochemical analysis of lingonberry (*Vaccinium vitis-idaea* L.) from different regions of China and their potential antioxidant and antiproliferative activities. *RSC Adv.*, **13**, 29438-29449. <https://doi.org/10.1039/D3RA05698H>
41. Vanlalveni C., Lallianrawna S., Biswas A., Selvaraj M., Changmai B., et al. (2021) Green synthesis of silver nanoparticles using plant extracts and their antimicrobial activities: A review of recent literature. *RSC Adv.*, **11**, 2804. <https://doi.org/10.1039/D0RA09941D>
42. Mittal A.K., Bhaumik J., Kumar S., Banerjee U.C. (2014) Biosynthesis of silver nanoparticles: Elucidation of prospective mechanism and therapeutic potential. *J. Colloid Interface Sci.*, **415**, 39-47. <https://doi.org/10.1016/j.jcis.2013.10.018>
43. Kumar B., Smita K., Cumbal L., Debut A. (2015) Green synthesis of silver nanoparticles using Andean blackberry fruit extract. *Saudi J. Biol. Sci.*, **24**, 45. <https://doi.org/10.1016/j.sjbs.2015.09.006>
44. Danielski R., Shahidi F. (2024) Phenolic composition and bioactivities of sea buckthorn (*Hippophae rhamnoides* L.) fruit and seeds: An unconventional source of natural antioxidants in North America. *J. Sci. Food Agric.*, **104**, 5553-5564. <https://doi.org/10.1002/jsfa.13386>
45. Rai M., Yadav A., Gade A. (2009) Silver nanoparticles as a new generation of antimicrobials. *Biotechnol. Adv.*, **27**, 76-83. <https://doi.org/10.1016/j.biotechadv.2008.09.002>
46. Ahmed S., Saifullah M., Ahmad B., Swami L., Ikram S. (2016) Green synthesis of silver nanoparticles using *Azadirachta indica* aqueous leaf extract. *J. Radiat. Res. Appl. Sci.*, **9**, 1-7. <https://doi.org/10.1016/j.jrras.2015.06.006>